Controllable porosity hydroxyapatite ceramics as spine cage: fabrication and properties evaluation

W. W. LU[1]*, F. ZHAO[1,2], K. D. K. LUK[1], Y. J. YIN[2], K. M. C. CHEUNG[1], G. X. CHENG[2], K. D. YAO[2], J. C. Y. LEONG[1]
[1]*Department of Orthopedic Surgery, University of Hong Kong, Hong Kong, People's Republic of China*
[2]*Research Institute of Polymer Materials, Tianjin University, Tianjin 300072, People's Republic of China*
E-mail: wwlu@hkusua.hku.hk

A procedure was designed to prepare porosity-graded hydroxyapatite (HA) ceramics simulating the bimodal structure of natural bone, which could be used to build a cage that would promote the reconstruction of the anterior column after vertebrectomy or corpectomy in tumor and trauma surgery. HA ceramics with controllable pore size distribution and porosity were developed by using chitosan and Poly(vinyl alcohol) (PVA) as the pore-forming agents. HA ceramics with worthwhile properties such as a wide range of volume porosity (10–50%) and pore size (nanometer to 400 μm) can be obtained from this method, which allows the fabrication of HA ceramics with desirable porous characteristics simulating the bimodal natural bone architecture expected to provide advantages for bony fusion in the intervertebral foramina. When coated with chitosan–gelatin network, the bending strength of the porous HA ceramics significantly improved. The polymer network coated porous HA have potential application in the construction of cages for spinal operations.

Introduction

The implantation of structural allografts and cages into the anterior column is helpful in correcting orthopedic deformities, including restoring sagittal plane misalignment in patients with spinal disorders. Much effort has been directed toward establishing the safety and effectiveness of the cages. Carbon fiber and metallic cages provide segmental stability [1], but the ability to provide a satisfactory environment for fusion with metallic cages has been questioned and stress shielding from subsidence can occur. Mesh cages filled with autogenous grafts have excellent interdigitation with the vertebral end plates, allowing for secure implantation. The vertical placement of such cages allows for optimization of autogenous grafting and intimal contact of the graft with the vertebral end plates within the cages, and leaves room for autogenous grafting outside of the cages. However, the supply of autologous tissue is limited and can lead to complications at the donor site [2, 3], and fresh-frozen allograft carries the risk of tissue rejection and disease transmission [4–6].

Due to its excellent biocompatibility and overall safety, and the fact that it has a chemical structure similar to the mineral found in hard tissues of the body, hydroxyapatite [HA: $Ca_{10}(PO_4)_6(OH)_2$], partially ionic substituted HA, and their composites have attracted much attention as materials suitable for repairing and substituting for hard tissues, and their clinical applications are gradually expanding [7–10]. Upon implantation, porous HA ceramics exhibit strong bonding to bone; the pores contribute to a mechanical interlock leading to a firmer fixation of the material with animal tissue. Graded porosity HA has a high-porosity portion (representing cancellous bone) that allows for good and fast bone ingrowth, and a low-porosity side (similar to cortical bone) that can withstand early physiological mechanical stress [11–13]. In addition, the porous structure also exhibits superior osteoconduction *in vivo* [14].

However, the strength of the porous HA implant materials tends to be related to macropore size. The current porous HA implants are brittle and may be susceptible to failure. Their application as cages is thus limited.

From the point of view of biomimetics, the purpose of this study was to prepare porous HA ceramics with bimodal pore size distribution and controllable porosity, and suitable mechanical strength for the potential application in the construction of cages for spinal operations. Even though the compressive strength matched the highest loading patterns in the spine, a weak bending strength for most of the HA materials has been recorded. Therefore, this study has focused on improved bending strength to match the requirement of the vertebrae body.

*Author to whom all correspondence should be addressed.

Materials and methods

HA with an average powder size of less than 75 μm was obtained from the Engineering Research Center of Biomaterials, Sichuan University, China.

Chitosan (mean molecular weight 8.0×105) was supplied by the Qingdao Medical Institute, China. It was purified as follows: The chitosan was dissolved in a 2% acetic acid aqueous solution until a homogeneous 1% chitosan solution was attained. The solution was neutralized with 10% NaOH solution to precipitate chitosan, and the chitosan obtained was washed with deionized distilled water and air-dried at 50 °C. The chitosan lumps were manually pulverized and sieved to obtain chitosan powders within a narrow range of sizes.

Poly(vinyl alcohol) (PVA) with a polymerization degree of 1400–1700 was supplied by the Beijing Chemical Factory (China). It was dissolved in water to form a homogeneous 7 wt % PVA solution.

Gelatin powder (bovine) was purchased from the Sigma Chemical Co. (St. Louis, MO). Glutaraldehyde and acetic acid were all chemical grade.

Preparation of HA block

To minimize the powder size, the HA was milled with a PVA aqueous solution in an agate-ball mill, which resulted in a powder size of 1–2 μm. After drying at 100 °C in air, the mixture was manually ground and sieved to get IIA aggregates of a size less than 40 μm.

The HA aggregates with addition of an appropriate content of chitosan powders were die compacted at 5.0 MPa and subsequently isostatically pressed at 108 MPa. The resulting series of blocks were calcined at a heating rate of 200 °C h^{-1} in air and soaked at 700 °C for 2 h, followed by furnace cooling. The blocks were then sintered at 700–1250 °C for 2 h and were cooled along with the furnace.

A control HA block without PVA was prepared by the same method.

Preparation of natural bone block

Pork ribs were selected as examples of natural bone. The ribs were cut into 1.5 cm pieces, and were then heated in a furnace at a heating rate of 200 °C h^{-1} in air and soaked at 500 °C for 2 h, followed by furnace cooling.

Preparation of chitosan-gelatin network coated HA block

The resulting porous HA ceramics were put in a vacuum container (over 720 mmHg) for 10 min, and then the samples were immersed in a 30% aqueous gelatin solution while the vacuum was maintained for another 5 min. The samples were then taken out and dried at 50 °C. In the following step, the samples were put in a vacuum container (over 720 mmHg) again for 10 min, and a solution of 7.5% aqueous chitosan and gelatin with glutaraldehyde was poured in to immerse the samples, while the vacuum was still maintained for another 5 min. The samples were then taken out and dried at 50 °C.

As the final step, the samples were treated with 50 ml of NaOH solution (10%) in 50 ml ethanol to neutralize the acetic acid, followed by washing with deionized distilled water to a pH of 7.0. The samples were then retreated with sodium borohydride ($NaBH_4$) solution to eliminate the unreacted glutaraldehyde.

Measurement of porosity distribution

A mercury porosimeter (Mercury Porosimeter, Micromeritics, USA) was used to test the pore size distribution of the samples.

Measurement of open porosity and volume density

Six smooth and crack-free samples were dried at 110 °C for 2 h and were then cooled to room temperature. After weighing (g_0), they were put in a vacuum container (over 720 mmHg) for 10 min and water was poured in to immerse the samples, while the vacuum was maintained for another 5 min. The vessel containing the samples was kept at atmospheric pressure for 15 min. Then the samples were picked out, their surface water was wiped off, and they were immediately weighed (g_1) in air. Subsequently, the specimens were weighed in water (g_2). The porosity and volume density were calculated according to the following expressions:

$$\text{Porosity} = (g_1 - g_0)/(g_1 - g_2) \times 100\%$$

$$\text{Volume density} = g_0/(g_1 - g_2)(\text{g cm}^3)$$

Bending strength

The HA plates were machined to fabricate the 3 point bending test specimens (25 mm × 4 mm × 4 mm) and tested at room temperature. Ten specimens were tested to failure on a servo-hydraulic materials testing machine (MTS 858 bionix machine, MTS System Inc., Minneapolis, MN, USA) at a crosshead speed of 0.5 mm min^{-1}.

Statistical analysis

The mean value and standard deviation were calculated for each group of 10 specimens. Analysis of variance and Student–Newman–Keuls multiple-range tests (SPSS) were used and statistical significance was considered if $P < 0.05$.

XPS analysis

X-ray photoelectron spectroscopy (XPS) measurements were carried out with an ESCA1600 (Philip, Japan) with monochromated Mg Ka (1253.6 eV) X-rays. The X-ray gun was operated at 23.5 eV, and the pressure was kept under 2.8×10^{-10} Pa. The sample preparations for XPS were conducted by the fracture surface of the coated HA block. Measurements started at a take-off angle of 30°. The binding energy scale was referenced to the main C1s peak attributable to contaminant hydrocarbon at 285.0 eV.

SEM observation

The morphologies of the HA and coated HA specimens were studied by scanning electron microscopy (SEM). The coated HA specimens were frozen in liquid nitrogen for 5 min and then broken for SEM observation. The fracture sections of the HA specimens were gold-coated and SEM observation was carried out using a Hitachi X-650 scanning electron microscope.

Results

Analysis of natural bone texture

Microstructural examination of natural bone by SEM reveals three categories of pores (Fig. 1). The first type is macropores, existing in the inner region of natural bone. Fig. 1(a) illustrates that the numerous macropores have a wide size distribution, and the biggest pore size is about 450 μm. The pores are interconnected in different directions as well. This interconnecting macroporous network allows tissue to infiltrate, and provides advantages for body fluid and blood circulation as well as allows the further supply of the nutrients and mineral ions that are necessary for functional and biological processes. The second type is located within the walls of the macropores (Fig. 1(b)) and is comprised of pores measuring approximately 0.5 μm in diameter, while the third type (Fig. 1(c)) averages 10 μm and corresponds to the pores situated in the cortical bone.

From the above analysis of natural bone microstructure, it can be concluded that natural bone contains pores of various sizes arranged in interconnected distribution patterns, growing in different directions. From the point of view of biomimetics, such bone characteristics should be taken into consideration in preparing bone substitute, and the pore size should be controled according to the practical requirements of the intended use of the substitute.

Influence of chitosan on microstructure of HA ceramics

Chitosan powders are flexible and tough at room temperature, and difficult to crush under high pressure. However, chitosan decomposes easily above 200 °C. Therefore, chitosan was chosen as the pore-forming agent.

The size of the chitosan incorporated in the green bodies strongly influences the microstructure of the

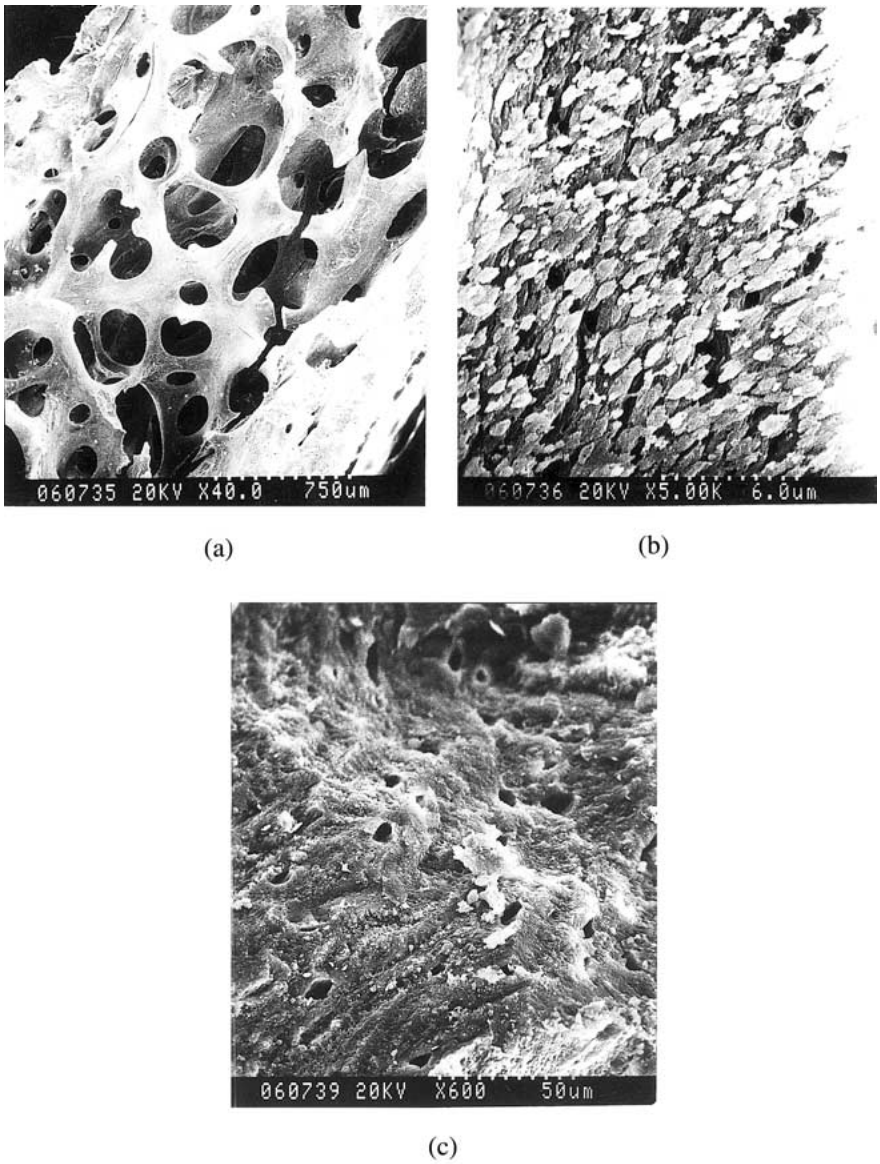

Figure 1 Micrographs of the fracture surfaces of the natural bone. (a) Inner part, (b) pore wall in inner part, and (c) cortical part.

sintered HA ceramics. HA ceramic develops porous features after appropriate heat treatment of the green bodies. Fig. 2 shows the influence of chitosan content on the morphology of HA ceramics. When the chitosan size is limited to 30–40 μm, ellipsoidal macropores, with a long axis of around 50 μm and a short axis close to 20 μm, have formed in different directions. Moreover, there are also numerous micropores in the pore wall. If the chitosan content is increased to 20%, the pores not only increase in number but also appear to have a tendency to interconnect, and the shape of the pores remains nearly stable. When the chitosan content is more than 30%, the pores increase both in number and in interconnectivity, and they turn into a honeycomb-like structure when the chitosan content reaches 40%.

Fig. 3 illustrates the morphologies of HA ceramics formed via sintering HA green bodies comprised of chitosan of different sizes but the same content (20%). The cross-sectional photographs show that the macropores distribute uniformly and randomly throughout the specimens, suggesting that the chitosan particles were well dispersed in the HA powders before die compaction. The pore size is enlarged when the chitosan diameter is increased, and the long axis of the ellipsoidal pores corresponds to different chitosan size; a 50 μm pore relates to a 30–40 μm chitosan diameter; 90 μm pore to 70–80 μm chitosan; and 400 μm pore to 300–360 μm chitosan.

The microporous structure of the macropore walls are shown in Fig. 4. One can see that the sizes of all the micropores are below 2 μm, independent of the diameters and contents of the chitosan incorporated in the green bodies. The formation of the micropores around the grain is attributed not only to the decomposition of PVA but also to the simultaneous diffusion and growth of sintered grains.

Influence of chitosan on properties of HA ceramics

The properties of the HA ceramics depend on the amount and size of the chitosan incorporated in the green bodies (Table I). When the chitosan content increases, the open porosity of the HA ceramic increases, and the volume density of the HA ceramic decreases. In addition, the bending strength deteriorates because of the enhancement of the porosity and the porous interconnection, which leads to weakened bridge connections between the

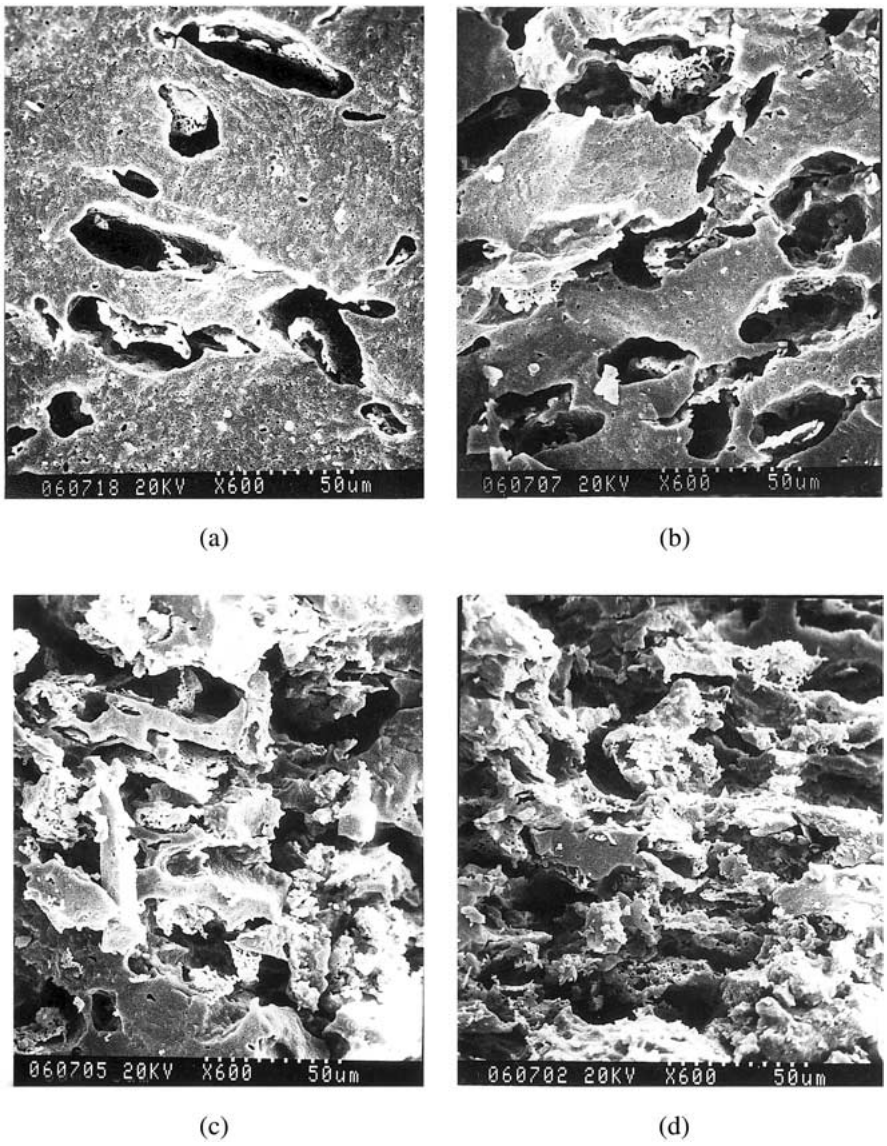

Figure 2 Micrographs of the fracture surfaces of HA ceramics sintered by HA green bodies with chitosan content of various weight ratios. (a) 10 wt %, (b) 20 wt %, (c) 30 wt %, and (d) 40 wt %.

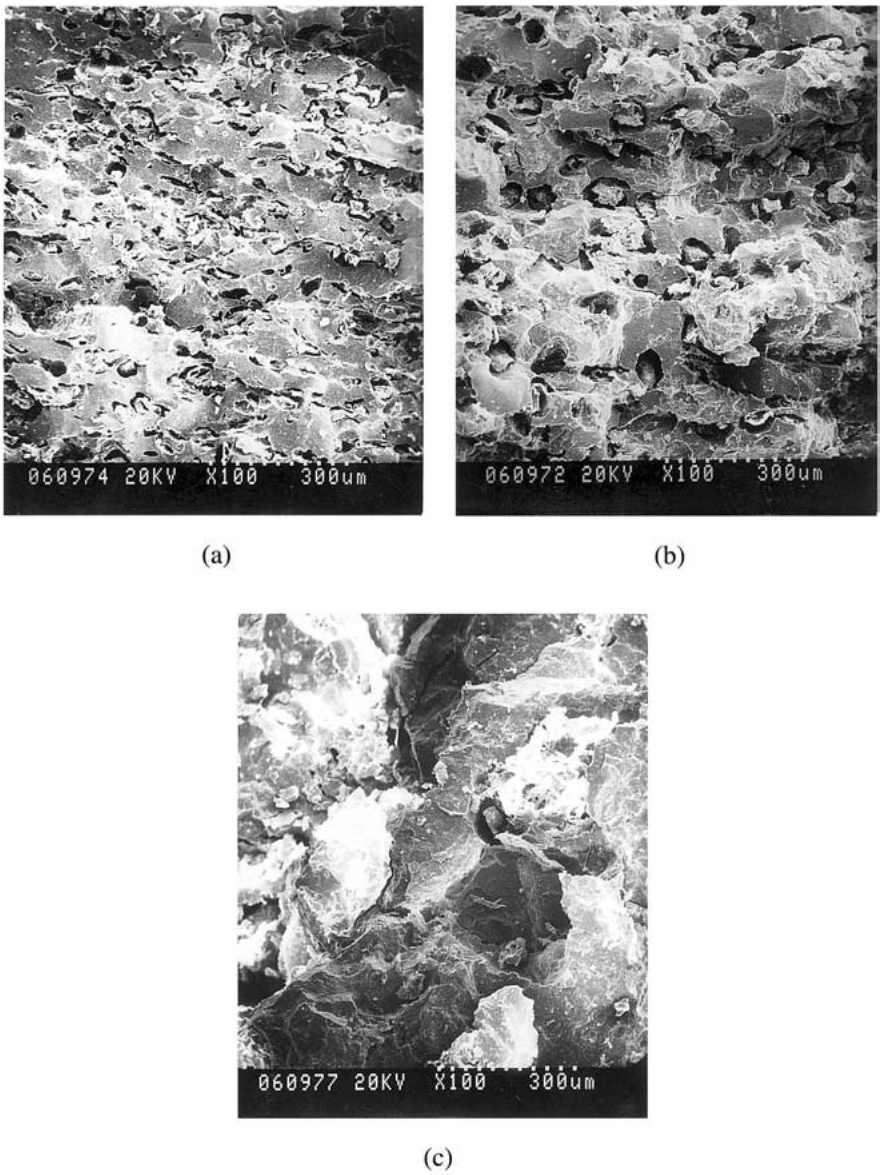

Figure 3 Micrographs of the fracture surfaces of HA ceramics sintered by HA green bodies with chitosan of different diameters. (a) 30–40 μm, (b) 70–80 μm, and (c) 300–360 μm.

HA crystal grains. When the chitosan content is constant, the volume densities and open porosities of the HA ceramics are nearly the same, while the bending strength significantly deteriorates when the chitosan size enlarges. It is thought that the content of the chitosan determines the porosity of the resulting HA ceramics, causing the densities to be similar. In addition, the bigger the size of the chitosan powders, the weaker is the packing of the fused HA powders. Consequently, the bending strength deteriorates with an increase in chitosan content.

Fabrication of HA ceramic

By comparing the microstructures and properties of the three kinds of HA ceramics, a balance is found when the chitosan content is 20–30 wt % in HA green bodies; at that level, the resultant HA ceramics have both an appropriate bending strength and suitable porosity.

According to the above results and the earlier analysis of the microstructure of natural bone, an HA ceramic was fabricated via sintering HA green bodies composed of 10 wt % 30–40 μm, 5 wt % 70–80 μm, and 300–360 μm chitosan. The properties of the HA ceramic are listed in Table II, which further prove the above conclusion.

Because mercury porosimetry allows characterization of the open porosity accessible to mercury, a bimodal pore size distribution pattern was shown to have been attained (Fig. 5). The curve shows that the ceramic has a wide pore size distribution, including macropores (> 10 μm), micropores (< 10 μm), and nanopores (0.008–0.03 μm). The wide pore size distribution would be expected to be favorable to the adhesion of cells and the infiltration of tissues.

Characterization of coated HA ceramic

The XPS survey spectrum for HA ceramic coated with gelatin at a 30° take-off angle clearly shows O, N, and C elements inside gelatin-coated HA ceramics. Peaks of N1s belonging to the gelatin also appear in the XPS spectrum of gelatin-coated HA ceramic, as shown in Fig. 6. 285, 287 and 288 eV is attributed to the chemical bonds of –C–H– and –C–C–, –C–O–, and –C–O–O– respectively. Therefore, the gelatin was successfully coated on the HA ceramics.

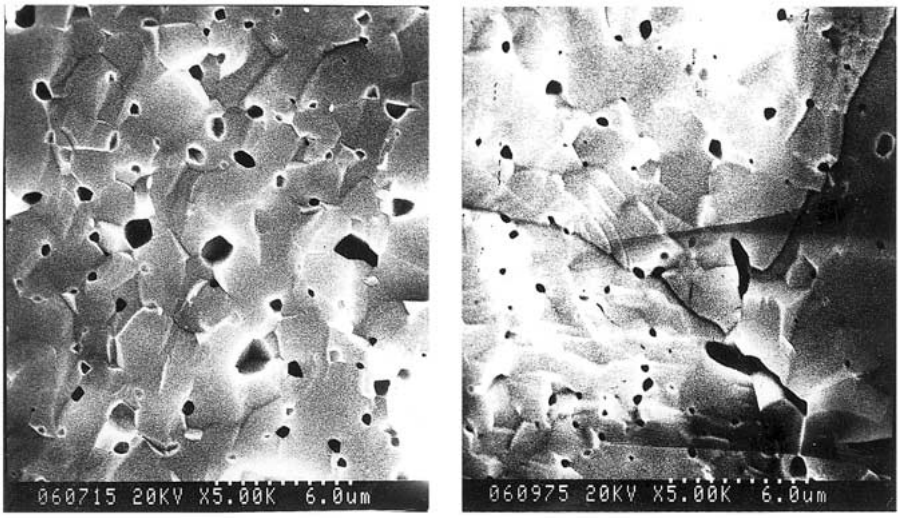

(a) (b) (c)

Figure 4 Micrographs of the fracture surfaces of HA ceramics sintered by HA green bodies with chitosan of different diameters and content. (a) 30–40 μm, 10%; (b) 70–80 μm, 20%; and (c) 300–360 μm, 30%.

TABLE I Influence of chitosan size and content on bending strength, volume density and open porosity of HA ceramics

Chitosan content (wt%)	Bending strength (MPa) for chitosan size of			Volume density (g/cm^3) for chitosan size of			Open porosity (%) for chitosan size of		
	30–40 (μm)	70–80 (μm)	300–360 (μm)	30–40 (μm)	70–80 (μm)	300–360 (μm)	30–40 (μm)	70–80 (μm)	300–360 (μm)
10	30.46 ± 2.23	17.77 ± 1.56	7.11 ± 0.82	2.64 ± 0.28	2.65 ± 0.25	2.61 ± 0.37	9.50 ± 1.12	14.14 ± 1.53	14.64 ± 1.33
20	15.39 ± 1.34	4.98 ± 1.12	0.42 ± 0.09	2.25 ± 0.09	2.20 ± 0.33	2.14 ± 0.25	25.30 ± 1.57	28.31 ± 1.21	29.70 ± 2.06
30	7.02 ± 0.78	1.64 ± 0.33	0.26 ± 0.07	1.63 ± 0.07	1.85 ± 0.42	1.88 ± 0.43	30.85 ± 1.36	39.44 ± 1.95	38.14 ± 1.83
40	2.62 ± 0.56	0.24 ± 0.05	—	1.64 ± 0.17	1.51 ± 0.16	—	47.02 ± 1.58	51.32 ± 2.23	—

Sintering condition: 1200 °C, 2 h.

TABLE II Bending strength, volume density and open porosity of the fabricated HA ceramic

Chitosan content (wt%)	Bending strength (MPa)	Volume density (g/cm^3)	Open porosity (%)
20	11.71 ± 1.22	2.19 ± 0.75	27.54 ± 1.29

Sintering condition: 1200 °C, 2 h.

Then the chitosan and gelatin network was recoated again on the surface of the gelatin-coated HA ceramics. Fig. 7 shows the fracture interface of the coated blocks. The organic network infiltrated into the HA ceramic and the interface bound tightly, leading to a firmer fixation of the material.

After being coated by the organic network, the bending strength of the HA ceramics significantly

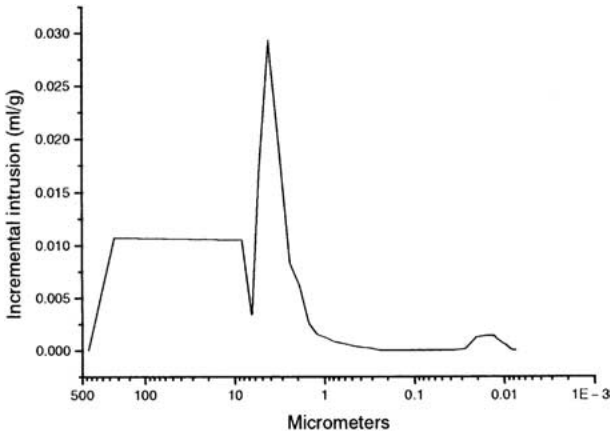

Figure 5 Pore size distribution of the HA ceramic.

TABLE III Comparison of the bending strength of the coated HA ceramics with original HA ceramics

HA ceramics prepared with chitosan size of (chitosan content 30 wt%)	Bending strength (MPa) for HA ceramics	Bending strength (MPa) for coated HA composites	Improvement (%)	*p*-value*
300–360 μm	0.26 ± 0.08	6.90 ± 1.58	2554	< 0.005
70–80 μm	1.64 ± 0.27	12.41 ± 1.64	657	< 0.01
30–40 μm	7.02 ± 1.89	18.35 ± 1.75	161	< 0.01

Sintering condition: 1200 °C, 2 h.
*Determined by comparison of coated HA to intact condition.

improved to the range of 6.9–18.35 Mpa (Table II). The coated HA block formed via sintering HA green bodies comprised of chitosan in the size range of 340–400μm showed a maximum improvement of 25.54 times.

Discussion

Depending on the location of injury and the void created at the time of surgical decompression, various anterior column reconstruction strategies have been used to restore spinal alignment and stability. Grafting materials traditionally have been taken from the autologous iliac crest and, in the case of multilevel reconstructions, the autologous fibula. Unfortunately, harvesting of autologous bone sources is fraught with several disadvantages including pain, neural injury, loss of structural support, risk of soft tissue herniation, and infection. Thus, alternative grafting sources are required. As such, the major contribution from this study is a porous HA with the strength of 7–18 Mpa which is similar to the strength of cancellous bone in the vertebrae body.

Porous HA is widely recognized as a substitute for bone graft because it is biocompatible, nontoxic, and non-inflammatory. Pores of a particular dimension and morphology play an important role and the presence of a pore size greater than 150 μm is essential for osteoconduction. Designing porous implant materials with a porosity gradient mimicking as much as possible the bimodal structure of bone (cortical and cancellous) and with a sufficient degree of interconnectivity is a most important challenge. However, the strength tends to

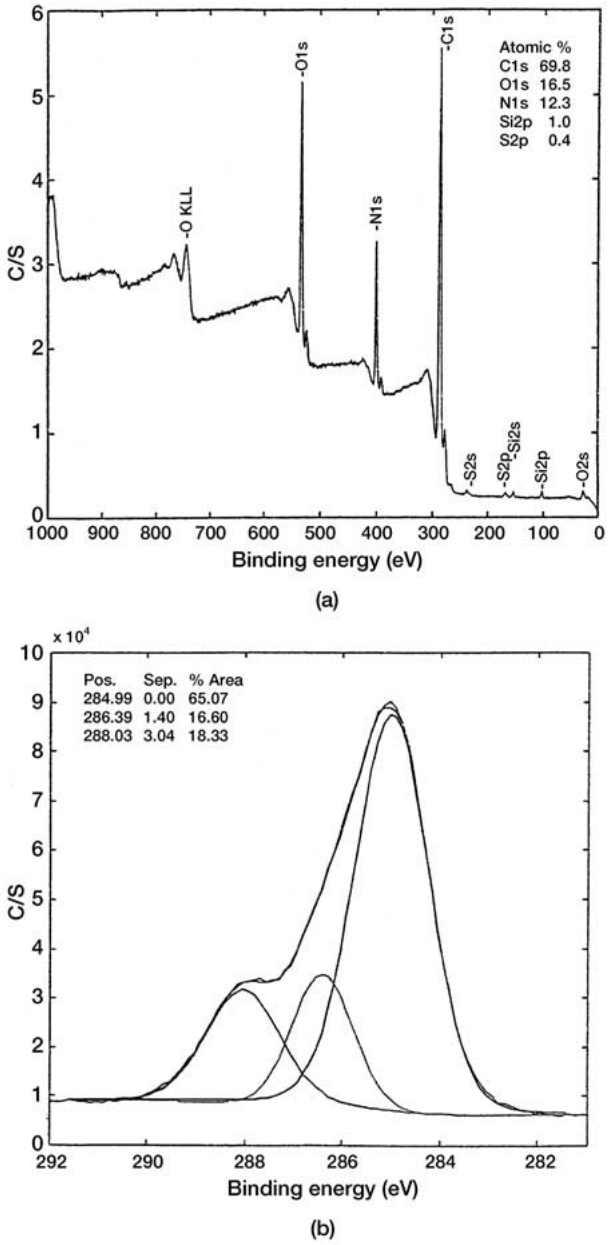

Figure 6 The XPS patterns of gelatin-coated HA ceramics. (a) The overall survey spectra, and (b) the survey spectra of C1s peak.

become sensitive to macropore size and volume at higher levels of porosity.

The microstructure of bioceramics plays an important role in bioresponse, because the porous structure of

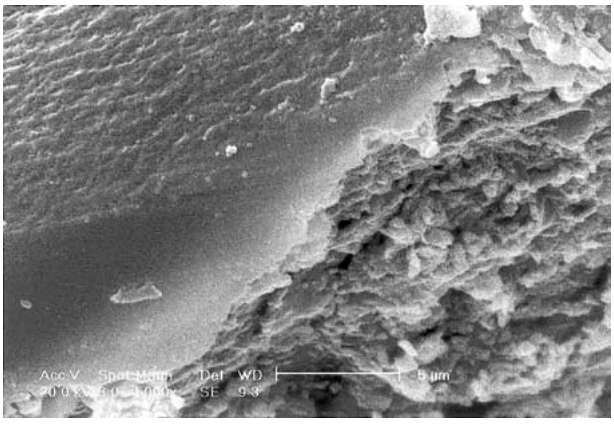

Figure 7 Micrograph of the fracture surfaces of chitosan–gelatin network coated HA ceramics.

implants serves as a scaffold for cell colonization, anchoring various tissue components, and bone ingrowth. Porous HA creates strong bonds to bone. The pores provide a mechanical interlock leading to a firmer fixation of the material. Bone tissue grows well into the macropores, increasing additionally the strength of the HA implant, while micropores on the macropore walls of the materials are important in osteoinduction [15].

To date, many methods have been adopted to prepare calcium phosphate ceramics with a porous morphology; for example, a porosity of 50–60% can be obtained by choosing an appropriate sintering temperature and a suitable heating rate [16]. Spongy cellulose is helpful in forming HA ceramics [13, 17]. The product with pore size distribution similar to natural bone ($< 10\,\mu m$, ~ 3 vo1 %; 10–150 μm, ~ 11 vo1 %; $> 150\,\mu m$, ~ 86 vo1 %) has high porosity (70–80%). Porous HA/tricalcium phosphate (TCP) materials were obtained using H_2O_2 as a pore-forming agent [18], where porosity may be modulated by H_2O_2 content and its evolution rate. However, the pore sizes are not uniformly distributed, and the biggest pore size is over 500 μm. The sol–gel method is a new route for preparing porous HA bioccramics with an average pore size of 0.2 μm and an open porosity of 15.5% [19]. HA ceramics with controled porosity have been manufactured by using the tape casting technique [20]. The final porosity is determined by the raw materials that react and release vapor during the sintering process. The hydrothermal hot-pressing (HHP) method [21] with the selection of the appropriate powder enables HA to be solidified at the low temperature and results in HA ceramics possessing a lamellar microstructure and high porosity.

Here, we used a simple method to prepare porous HA with high porosity and a bimodal pore structure similar to that of the natural bone. To improve the bending strength of the HA ceramics, we used the chitosan-gelatin network to coat the porous HA ceramic surface. Based on a biomimetic approach, we have prepared a composite of HA and a cross-linked network of chitosan and gelatin with glutaraldehyde [22]. Gelatin, as a partially denatured derivative of collagen, has very good biocompatibility and is biodegradable. Chitosan is a biocopolymer comprising of glucosamine and *N*-acetylglucosamine, obtained by deacetylation of chitin. It has been reported to be safe, hemostatic, and osteoconductive, and to promote wound healing [23, 24].

In this way, the strength of the HA ceramics was significantly improved. When used as cages in spinal surgery, coated HA ceramics are expected to provide strong mechanical support during the early period of implantation. Then with the biodegradation of the organic network, the new bone tissue gradually grows into the pores of the HA ceramics and effective bonding may form between the HA ceramics and bone tissue.

5 Conclusions

In this approach a novel method was developed to design HA ceramics with a controllable pore size distribution and porosity, depending on the characteristics of the introduced polymer powder chitosan, which was used as the pore-making agent. The HA ceramics obtained had a bimodal pore size distribution, which contain macropores ($> 10\,\mu m$), micropores ($< 10\,\mu m$), and nanometer pores (0.008–0.03 μm), and also had a wide range of volume porosity (10–50%). The bending strength of HA ceramics was significantly improved after the surface was coated by the chitosan-gelatin network.

Acknowledgments

This study was supported by grants from the Hong Kong Research Grant Council (RGC: HKU7249/99M) as well as the National Science Foundation of China (59883002).

References

1. S. BORIANI, R. BIAGINI, S. BANDIERA, A. GASBARRINI and L. F. DE, *Orthopedics* **25** (2002) 37.
2. E. D. ARRINGTON, W. E. SMITH, H. G. CHAMBERS, A. L. BUCKNELL and N.A. DAVIDINO, *Clin. Orthop. Rel. Res.* **329** (1996) 300.
3. E. M. YOUNGER and M. W. CHAPMAN, *J. Orthop. Trauma.* **3** (1989) 192.
4. A. MIZUTANI, T. FUJITA, S. WATANABE, K. SAKAKIDA and Y. OKADA. *Int. Orthop.* **14** (1990) 243.
5. J. R. MOORE, T. W. PHILLIPS, A. J. WEILAND and M. A. RANDOLPH, *J. Orthop. Res.* **1** (1984) 352.
6. J. T. MELLONIG, A. B. PREWETT and M. P. MOYER, *J. Periodont.* **63** (1992) 979.
7. I. REHMAN and W. BONFIELD. *J. Mater. Sci.: Mater. Med.* **8** (1997) 1.
8. M. J. DALBY, L. DI SILVIO, N. GURAV, B. ANNAZ, M. V. KAYSER and W. BONFIELD, *Tissue. Eng.* **8** (2002) 453.
9. M. J. DALBY, L. DI SILVIO, E. J. HARPER, W. BONFIELD, *Biomaterials* **23** (2002) 569.
10. Y. DOI, T. SHIBUTANI, Y. MORIWAKI, T. KAJIMOTO and Y. IWAYAMA, *J. Biomed. Mater. Res.* **39** (1998) 603.
11. L. L. HENCH, *J. Am. Ceram. Soc.* **74** (1991) 1487.
12. S. K. RITTER. *Chem. Eng. News* **28** (1997) 27.
13. A. TAMPIERI, G. CELOTTI, S. SPRIO, A. DELCOGLIANO and A. FRANZESE, *Biomaterials* **22** (2001) 1365.
14. N. TAMAI, A. MYOUI, T. TOMITA, T. NAKASE, J. TANAKA, T. OCHI and H. YOSHIKAWA, *J. Biomed. Mater. Res.* **59** (2002) 110.
15. H. YUAN, K. KURASHINA, J. D. BRUIJN, Y. LI, K. GROOT and X. ZHANG, *Biomaterials* **20** (1999) 1799.
16. K. HINO, *Metal (in Jpn.)* **68** (1998) 121.
17. M. FABBRI, G. C. CELOTTI and A. RAVAGLIOLI, *Biomaterials* **16** (1995) 225.
18. J. ZHANG and X. ZHANG. *J. Mater. Sci.: Mater. Med.* **5** (1994) 243.
19. P. LAYROLLE, A. ITO and T. TATEISHI. *J. Am. Ceram. Soc.* **81** (1998) 1421.
20. I. H. ARITA, D. S. WILKINSON, M. A. MONDRAGON and V. M. CASTANO. *Biomaterials* **16** (1995) 403.
21. K. HOSOI, T. HASHIDA, H. TAKAHASHI, N. YAMASAKI and T. KORENAGA. *J. Am. Ceram. Soc.* **79** (1996) 2771.
22. Y. J. YIN, F. ZHAO, K. D. YAO, X. F. SONG, W. W. LU and J. C. Y. LEONG. *J. Appl. Polym. Sci.* **77** (2000) 2929.
23. A. RAZANIA and K. E. HEALY, *Biotechnol. Prog.* **15** (1999) 19.
24. Y. J. PARK, Y. M. LEE, S. N. PARK, S. Y. SHEEN, C. D. CHUNG and S. J. LEE, *Biomaterials* **21** (2000) 153.

Received 24 December 2002
and accepted 3 June 2003